

Second-harmonic generation of $\lambda \sim 1 \mu\text{m}$ enhanced by intersubband transitions of GaN/AlN quantum wells

L. Nevou, M. Raybaut, M. Tchernycheva, F. Guillot, E. Monroy, F. Julien, A. Godard, and E. Rosencher

Abstract— We report on the observation of resonant enhancement by intersubband transitions of the second-harmonic generation of $1 \mu\text{m}$ radiation in GaN/AlN quantum wells grown on AlN/*c*-sapphire templates. The quantum wells with a nominal well thickness of 10 monolayers have been investigated in terms of intersubband linear and nonlinear optical properties. A strong increase of the second harmonic conversion is observed at a pump wavelength of $2 \mu\text{m}$, which is attributed to double-resonance enhancement of the nonlinear susceptibility by intersubband transitions. The second-order susceptibility at resonance is of the order of 114 pm/V in good agreement with calculations and corresponds to a factor of 4 enhancement with respect to bulk GaN.

Index Terms—Second harmonic generation, intersubband transitions, nitride quantum wells.

I. INTRODUCTION

In semiconductor quantum wells (QWs), the second-order non-linear susceptibility is known to be strongly enhanced, when the waves are in close resonance with intersubband transitions (ISB) [1]. However, since the second-order nonlinear susceptibility is identically zero in a potential with an inversion symmetry, an asymmetric potential is required to benefit from the ISB resonance enhancement. Resonant second harmonic generation (SHG) in the mid-infrared spectral range has been reported in various material systems such as GaAs/AlGaAs, AlInAs/GaInAs or SiGe/Si. The asymmetric potentials were provided either by bias application, step-like composition or asymmetric coupled QWs [2,3]. In contrast to these materials, hexagonal-phase GaN/AlGaIn QWs grown along the *c*-axis naturally exhibit an asymmetric saw-tooth potential, which arises from the piezoelectric and spontaneous polarization discontinuity between the well and barrier materials. In addition, the band offset

offered by nitride heterostructures is large, up to $\approx 1.75 \text{ eV}$ for GaN/AlN [4], which allows ISB transitions to cover the near-infrared spectral domain [4-7]. Large second-order nonlinear susceptibilities at near-infrared wavelengths were predicted in GaN/AlGaIn QWs due to ISB resonant enhancement [8].

II. RESULTS AND DISCUSSION

Here we report on the observation at room temperature of ISB resonant enhancement of SHG in GaN/AlN QWs grown on AlN/*c*-sapphire template. Under double-resonance conditions with the e_1e_2 and e_2e_3 ISB transitions, the conversion is 16 times more efficient in the QW sample with respect to bulk GaN [9].

The sample was grown by plasma-assisted molecular beam epitaxy at 720°C . The substrate consists of *c*-sapphire with a $1 \mu\text{m}$ thick AlN buffer layer. The active region contains 200 periods of nominally 10 monolayer-thick GaN wells (1 ML = 0.26 nm) separated by 3 nm thick AlN spacer layers. The sample is non-intentionally doped. The electron concentration is provided by residual doping.

The sample was investigated using Fourier transform infrared spectroscopy. Figure 1 shows the p-polarized absorption spectrum of the QW sample measured in a multi-pass waveguide configuration with 15 total internal reflections. No absorption is observed for s-polarized light. A p-polarized absorption is peaked at $1.95 \mu\text{m}$ wavelength. The ripple visible in the spectrum is related to ML fluctuations of the well thickness during the growth of the QW stack as shown in Ref [4]. More precisely, each peak is ascribed to the e_1e_2 ISB absorption of wells with a thickness equal to 9, 10 and 11 ML, respectively. The full width at half maximum of each peak is 42 meV . An additional absorption peak is observed at $1.05 \mu\text{m}$ wavelength. This peak is attributed to the low oscillator strength e_1e_3 ISB absorption [4]. Based on measured absorption magnitude, we estimate the electron concentration in the wells to be $1.05 \times 10^{12} \text{ cm}^{-2}$.

The inset of Fig. 1 illustrates the pumping scheme for SHG. The SHG measurements were performed at room temperature using optical pumping by a pulsed OPO tunable in the wavelength range of $1.9\text{-}2.3 \mu\text{m}$. A $\lambda/2$ plate is used for rotating the polarization of the output beam. The output beam is focused using a CaF_2 lens with 5 cm focal length onto the sample set at Brewster's angle. The spot diameter is measured to be $300 \mu\text{m}$. The transmitted beam is then filtered by a dichroic filter to eliminate the pump radiation transmitted

Manuscript received March 15, 2007. This work was supported by the European FP6 NitWave program (contract IST #04170).

L. Nevou, M. Tchernycheva, F. H. Julien, are with the Institut d'Electronique Fondamentale, UMR 8622 CNRS, Bat. 220, Université Paris-Sud, 91405 Orsay, France (corresponding author L. Nevou phone: 33169154051; fax: 33169154115; e-mail: laurent.nevou@ief.u-psud.fr).

M. Raybaut, A. Godard, E. Rosencher are with the Office National d'études et de Recherches Aéropatiales, Chemin de la Hunière, F-91761 Palaiseau, France

F. Guillot, E. Monroy are with Equipe mixte CEA-CNRS-UJF Nanophysique et Semiconducteurs, DRFMC/SP2M/PSC, CEA-Grenoble, 17 Rue des Martyrs, 38054 Grenoble Cedex 9, France.

through the sample. Detection is performed by an avalanche silicon photodiode and a box-car integrator.

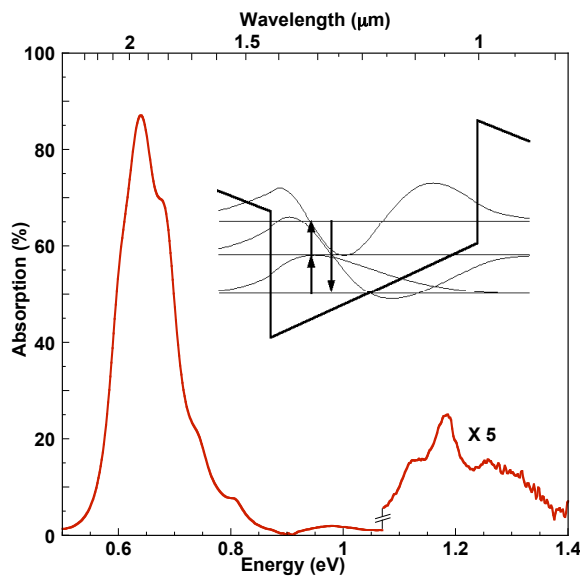


Figure 1: 300 K absorption spectrum in multipass waveguide configuration of the quantum well sample.

The Figure 2 shows the power emitted by the QW sample at 1 μm wavelength versus the peak pump power. The pump wavelength is 1.98 μm and the pump beam is p-polarized. The emitted power closely follows a quadratic law with pump power, as expected for a SHG process. The signal vanishes either when the pump beam is s-polarized or when the sample is rotated at normal incidence, as expected from ISB polarization selection rules.

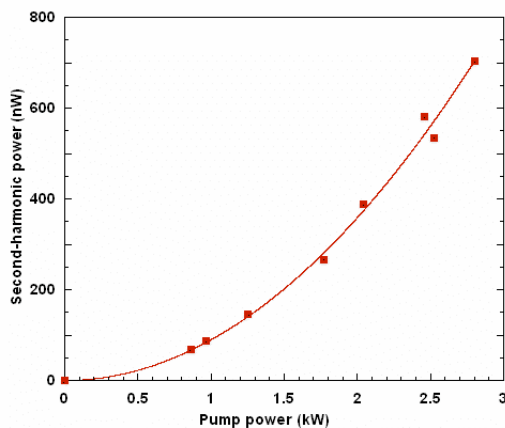


Figure 2: Second-harmonic power vs pump power for the QW sample (curve is a quadratic fit).

Figure 3 presents the squared modulo of the second-order non linear susceptibility versus the pump energy for the QW sample (red curve) in addition to the absorption spectrum at Brewster angle of incidence. The second-harmonic power exhibits a strongly resonant behavior with conversion efficiency peaked at 2.0 μm wavelength. The full width at half maximum of the resonant peak is 18 meV, which corresponds

to a reduction by a factor 2.33 of the linewidth with respect to the ISB absorption. This value is close to the theoretical value, 2.39, characteristic of a double-resonance enhancement of the second-harmonic process [10]. Separate experiments performed on a reference sample (3.5 μm thick GaN layer) do not show any resonant enhancement in the investigated pump wavelength range (blue curve).

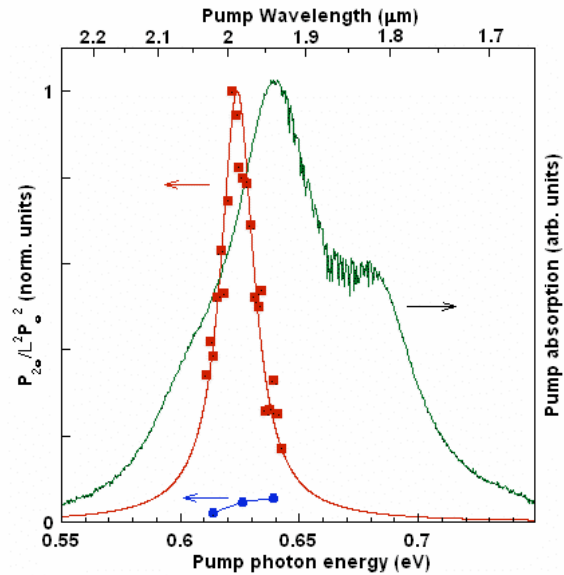


Figure 3: Second-harmonic power divided by the squared pump power and by the squared interaction length versus pump wavelength. The red squares (blue circles) are measurements for the QW sample (3.5 μm thick GaN layer). The red curve is a Lorentzian fit. The absorption spectrum at Brewster's angle of incidence is indicated in green.

For the same thickness of the active region, the conversion at a pump wavelength of 2.0 μm is found to be 16 times more efficient in the QWs with respect to bulk GaN, which is a consequence of the enhanced value of the nonlinear susceptibility. Based on the SHG power measurements, the value of $\chi_{zzz}^{(2)}$ is deduced to be 114 pm/V for the QW sample in close agreement with the calculated value of 135 pm/V. The value of $\chi_{zzz}^{(2)}$ at resonance could be further enhanced by increasing the electron density in the wells.

These results open prospects for compact size optical parametric oscillators, operating at near infrared wavelengths.

REFERENCES

1. M. K. Gurnick and T.A. DeTemple, *IEEE J. Quantum Electron*, **QE-19**, 791 (1983).
2. M. M. Fejer *et al.*, *Phys.Rev.Lett.* **62**, 1041 (1989).
3. P. Boucaud, *et al.*, *Appl. Phys. Lett.* **57**, 215 (1990).
4. M. Tchernycheva *et al.*, *Phys. Rev. B* **73**, 125347 (2006).
5. C. Gmachl *et al.*, *Appl. Phys. Lett.* **77**, 3722 (2000).
6. K. Kishino *et al.*, *Appl. Phys. Lett.* **81**, 1234 (2002).
7. N. Iizuka *et al.*, *Appl. Phys. Lett.* **81**, 1803 (2002).
8. A. Liu *et al.*, *Appl. Phys. Lett.* **76**, 333 (2000).
9. L. Nevou *et al.*, *Appl. Phys. Lett.* **89**, 151101 (2006).
10. E. Rosencher and P. Bois, *Phys. Rev. B* **44**, 11315 (1991).